International Journal of Engineering Trends and Technology
ISSN: 2231 – 5381 / https://doi.org/10.14445/22315381/IJETT-V70I11P222
Volume 70 Issue 11, 204-210, November 2022
© 2022 Seventh Sense Research Group®

Original Article

Thermo-Mechanical Analysis of Friction Drilling Process on Al 6061-T6 with Fem Analysis

Nimmagadda Srilatha [1], Balla Srinivasa Prasad [2]

[1]*Department of Mechanical Engineering, VNR VJIET, Hyderabad India.*
[2]*Department of Mechanical Engineering, GITAM Institute of Technology, Visakhapatnam, India.*

[1]*Corresponding Author : srilatha.nimmagadda321@gmail.com*

Received: 08 August 2022 Revised: 04 November 2022 Accepted: 16 November 2022 Published: 26 November 2022

Abstract - *The stirring is caused by friction. Non-conventional hole-creation processes include drilling. No chips are formed since the revolving conical tool is concerned with entering a drill hole and making a bushing both above and below the workpiece in one single phase. A revolving conical tool causes friction between a drill bit and a piece of material, causing the material to soften, penetrate, and form a bushing. Deform-3D software is used to construct three-dimensional objects for this study, which then performs a finite element analysis to determine workpiece deformation and big strain during friction stir drilling. The thermal and mechanical characteristics are determined via explicit dynamic analysis with adaptive meshing. We cannot measure the flow of work material deformation or stress and strain distribution during friction stair drilling with our hands. Therefore we use a finite element analysis to simulate this process. Modeling the tool and the workpiece in CATIA software is utilized for the study. The melting point of the work item has been determined using FEM findings.*

Keywords - *Friction drilling, CATIA, Deform-3D, Explicit dynamic analysis, Temperature.*

1. Introduction

Drilling is a significant part of machine operations, accounting for almost all machining operations. A drill tool's lifespan is limited because of the high temperatures generated during the drilling operation, which dulls it. One of the biggest challenges in the automotive industry is finding the most effective and simplest technique to connect or assemble two components, such as tubes, sheet metal, and thin-walled components. Although weld nuts, threaded inserts, and J nuts are often employed to solve these issues, there are a few drawbacks to this method that include the weight and expense, as well as the compromise in the quality and the inclusion of external components. For all these situations, friction stair drilling is the only viable option. Fractional and flow drilling are all terms that refer to the same process known as friction drilling [1]. Due to chipless hole making due to, without smoke friction, drilling has become more popular. In this method, the tool uses the heat generated between the rotating conical tool and the workpiece to soften the work material to create a hole in the workpiece. Similarly, it creates a bushing and boss at the up and down part of the work material to strengthen the hole. A rapid increase in temperature causes plastic deformation to occur in the work material at the hole area so that the material contributes towards to bushing shape while increasing hole length. During this high temperature, material properties and microstructure changes occur in friction drilling.

Bushing length is three times the work material thickness, giving a better clamping load and threading. [22]. various material thicknesses, feed and speed, are used to investigate the height of bushing and thickness for AISI 1015 with the help of the friction drilling process. RSM technique wear used for speed and feed optimization for various material thicknesses. When rotational speed increases, there is an increment in bushing height and gradual decreases in bushing width. CMM is used to measure the dimension of the friction drilling hole (3) material; various stages of the friction drilling process are given below in figure 1.

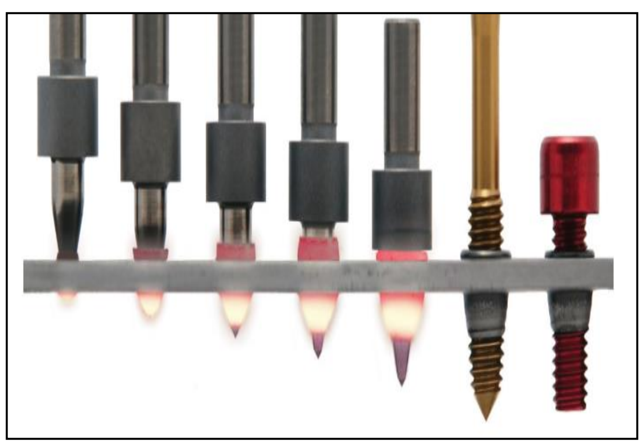

Fig. 1 Various stages of the Friction Drilling Process.

This is an open access article under the CC BY-NC-ND license (http://creativecommons.org/licenses/by-nc-nd/4.0/)

Optimal strategies are created for controlling the feed in FD. Two strategies are followed: general linear variable feed at each individual stage, adaptive control feed rate, and correlation between torque and force are considered with respective relation to speed and feed rate. Based on this sensor, less optimization was created to protect long-term and excessive loads of tools and drives (4) from improving the material flow with respective compression, yield in shear and instant of single & variable coefficient of friction to develop the new model for friction drilling, coefficient of friction and shear stress cannot be able to measure directly with time dependence. (5). These tungsten carbide bits with coated and uncoated are used to produce a hole on AISI 304 with TiAIN and AlCrN are coated to drill bit with the help of the PVD method at various spindle speeds. The highest temperature was produced with an AlCrN-coated tool with low axial force and tool wear. (6). Optimal process parameters for FD on SUS 304 stainless steel were investigated with varying speed and feed rates to correlate with output parameters like surface roughness and bushing length using grey relational grade. Maximum tool wear can be eliminated in the friction drilling process, and surface integrity has improved in the friction drilling hole. (7). with a varying material thickness of stainless steel to optimize the machining conditions of FD at different speeds are analyzed. To compute torque and thrust force and other hand dimensional errors and microstructures of friction drilling hole are analyzed. (8). In this friction drilling study, IN-713LC, a nickel-based superalloy, investigated work material properties, including surface roughness, roundness, and hardness. More hardness is founded nearer to the FD hole wall, and hardness is decreased with increasing hole distance. Increasing the feed rate leads to greater roundness and better surface roughness. (9). FCAR does not affect the bushing height much. Most Friction drilling applications are sheet metals and Driveshaft Brake systems (10). A finite element analysis was created to identify the material flow of the friction drilling process for AISI 1020 carbon sheets of steel. At the same time, torque and thrust force can also be determined with the friction drilling tool of tungsten carbide material. Moreover, compared with FEM analysis (11). Compression between experimental and numerical analysis was done for output parameters of friction drilling, like torque, force, and temperature. For that, FEM analysis was performed with the help of Deform- 3D simulation software. (12). Effect of bushing shape and surface roughness with various respective speeds and feed rates are calculated for Al6061-T6 alloy of 3mm thickness. Optimal process parameters are optimized by using Gray Relation Analysis. (13). Soundararajan et al. (14), Chao et al. (15) Schmidt and Hattel (16) are researching to create modelling of the Friction stair welding process. There are few applications of friction drilling.

2. Experimental Methodology and Materials

In this Friction drilling process, Al6061-T6 Alloy was used as workpiece material. The region behind this is Al6061-T6 Alloy, widely used in most industrial applications such as Military and commercial bridges, Aerospace applications, Shipbuilding operations, Boiler making etc. The chemical composition of the Al6061-T6 Alloy workpiece in terms of weight percentages is Aluminium 95.85%, Zi 0.25%, Mg 1.2%, Ti 1.15%, Si 0.8%, Co 0.4%, Mag 0.15%, and iron 0.7%. The main alloying elements are Silicon and Magnesium, and the melting temperature of Al6061-T6 alloy is 580-650 °C. Hear Tungsten carbide (WC) and High-Speed Steel (HSS) were selected for friction drilling tools, and the dimensions are as follows such as diameter d=8mm; centre length (h_c) = 2mm; conical length (h_n) =6.6mm; cylinder length (h_1) = 30mm; shoulder Length (T) =10mm; shank length (L) =30mm; centre angle = 90˚ and conical angles ø is 36 ˚.

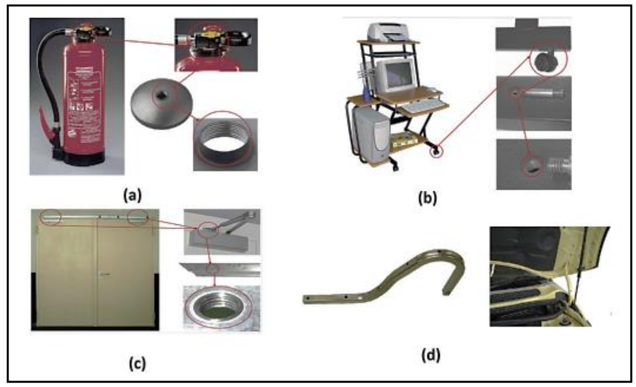

Fig. 2 Applications of Friction Drilling Process

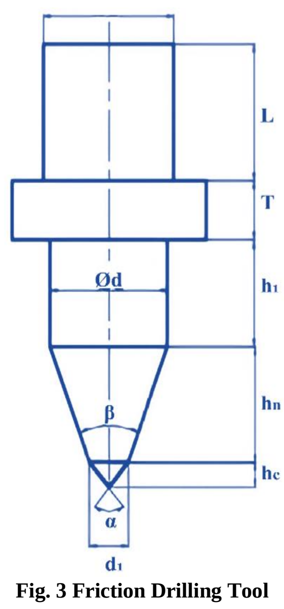

Fig. 3 Friction Drilling Tool

3. Finite Element Analysis

The method employed for friction stair welding is suitable for friction stair drilling. Because both friction drilling and the FSW process will involve a similar principle, in both processes, high temperature and friction will be generated at the tool and workpiece interface with the rotating tool. It results that the dissimilar materials will be joined in FSW, and holes with bush and boss will happen in the friction drilling process. The only important disparity to happen is in both FD and FSW. (17). Deform-3D software was selected to simulate the friction drilling process for Al 6061-T6 alloy work material. DEFORM-3D and Arbitrary Lagrangian–Eulerian (ALE) formulation have been chosen for simulation. For metal forming, heat treatment problems and different forming operations, finite element analysis-based software is selected to analyzed material flow; industries of scientific-forming technologies corporation developed this. In this FEM analysis, some succeeding operations are utilized to simulate FD and FSW. 1. The work piece's model is considered rigid visco-plastic. 2. Tool of the friction drilling process was considered rigid. 3. Because of radiation, heat loss was small. 4. Constant Coefficient of Friction was considered at the tool and workpiece interface. (18).

3.1. Mesh and Boundary Conditions

Deform-3D simulation software has been used for FEM analysis of the friction drilling process. Simulation parameters are presented in Table2 for the FD process. The work material model has dimensions of 50mm diameter and 3mm thickness. With the help of the DEFORM-3D software workpiece model was created. The workpiece lateral surface was held in all three directions, i.e. X, Y and Z directions, to ignore the oscillation during the FD simulations process. Hear CATIA-V5 software is used to develop 3D modelling of friction drilling tools and convert 3D model files to STL format of FD drill. After converting the 3D model to an STL file imported to DEFORM-3D simulation software. In this software, for the simulation process, materials are chosen those are HSS, WC is the tool material, and Al6061-T6 alloy is the work material. In Z-direction, rotational speed (S) 1980rpm and feed rate (F) 0.08 mm/rev are applied towards to friction drilling process.

3.2. Governing Equations for the Friction Drilling Process

For the friction drilling process, the thermos-mechanical study was incorporated successfully by deriving some of the following equations: momentum, continuity, and energy conservation. These equations can be solved with the help of material properties. The mechanical properties have been maintained based on the normality principle (19).

$$\delta_t = 2 d_a \mu \tag{1}$$

$$d_r = \dot{\epsilon}\left[\frac{\partial \overline{\sigma_e}}{\partial \delta_{time}}\right] = 1.5\left[\frac{\dot{\epsilon}}{\partial \overline{\sigma_e}}\right] \quad \delta_t = \frac{\delta_{time}}{2\mu} \tag{2}$$

$$\overline{\sigma_v} = \sqrt{1.5}\delta_{time}.\delta_{time} \qquad \dot{\epsilon} = \sqrt{0.6667 d_{r.}}\, d_R \tag{3}$$

Where stress deviatoric $\delta_{t,}$ yield stress $\overline{\sigma_e}$, Effective strain $\dot{\epsilon}$, and viscosity. Where viscosity is in terms of strain $\dot{\epsilon}$ and temperature T. Viscosity μ ($\dot{\epsilon}, T$), the yield stress $\overline{\sigma_e}(T)$ is in terms of temperature (T).

$$\mu = 0.33\left[\frac{\overline{\sigma_e}}{\dot{\epsilon}}\right] \tag{4}$$

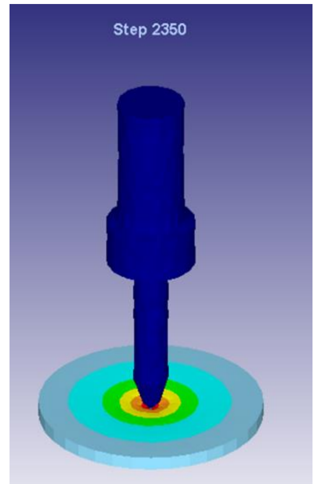

4(a)

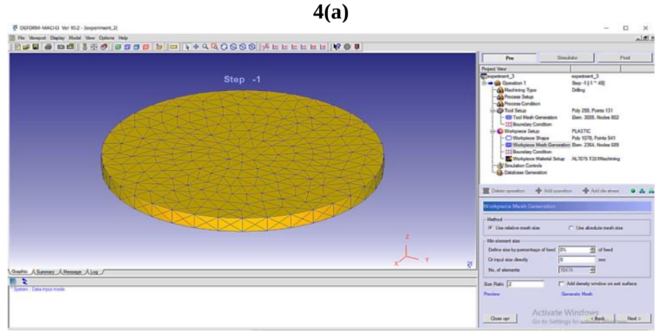

4(b)

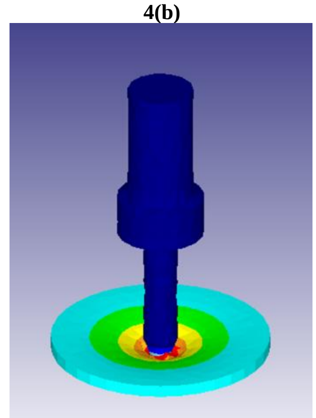

4(c)

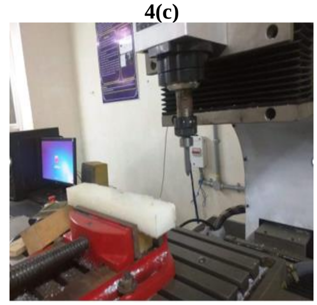

4(d)

Fig. 4 (a) Mesh tool (b) Meshed work material (c) Initial Stage of Tool & (d) Experimental setup

Based on the Conservation of momentum law [18]

$$\nabla.\sigma_a + \rho a = \rho\left[\frac{dV}{dtemp}\right] \quad (5)$$

Where ρ, σ_a, a, t and V are the density, stress, acceleration, time, and velocity vector. Derivatives of material time $\frac{d}{dtemp}$. Here the continuity equation for the FD process is given following [18].

$$V.\nabla_\rho = -\frac{\partial\rho}{\partial temp} \quad (6)$$

According to the law of energy conversion [18],

$$\rho C_s \frac{dT}{d_{temp}} = \nabla.\left(K_{temp} \nabla T\right) + q_{gen} \quad (7)$$

Where specific heat, thermal conductivity, and generation of heat are c_s, K_t , andq_g. $K_t(T)$ as thermal conductivity being in terms of temperature. [18].
Generation of heat can be given as

$$q_g = C_{fa}.\delta_{time.}d_{a.} \quad (8)$$

Where C_{fa} the corrosion factor, the surrounding temperature is T_a.
From Equation (7) heat transfer coefficient can be obtained by

$$h_c = \frac{K_{temp}\nabla T}{(T-T_a)}. \quad (9)$$

4. Results and Discussion

Generally, work material is directly influenced by feed rate and speed in the friction drilling process. So it is important to choose input parameters like speed and feed rates in the friction drilling process. In this FD process, it is impossible to measure stress, strain and deformation of work material and the physical structure of the workpiece.

To visualize all these parameters, DEFORM-3D software has been chosen in this work. With the help of this software, FEM simulation is done to identify material flow stress and strain in the workpiece. [19][24]. with the varying speeds and feed rates in friction drilling, the stress, strain, and material flow could be effectively found where Al6061-T6 alloy is the work material and Tungsten carbide and HSS as tool materials.

The primary feasibility of the FEM simulation is the capability to gain accuracy for the friction stir drilling workpiece of stress, strain, deformation of work material and temperature distribution, which are unable to measure experimentally. Figures 5, 6, 7, 8, & 9 show stress, strain, temperature, and material deformation at various speeds and feed rates with different tool materials.

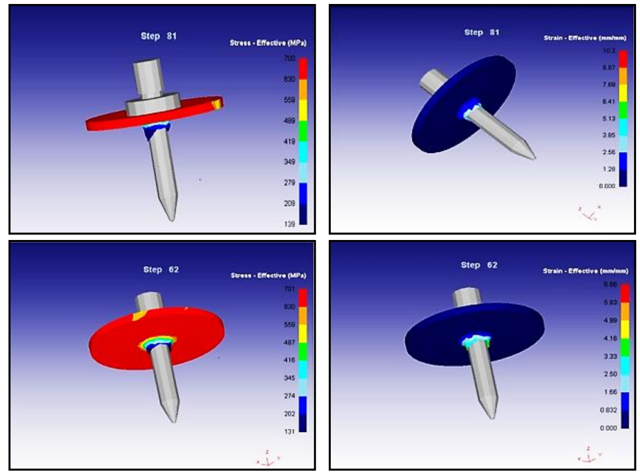

Fig. 5 Stress, strain analysis of HSS tool on AL6061-T6 workpiece at Feed 0.08mm/rev and Speeds 1980 & 1250rpm

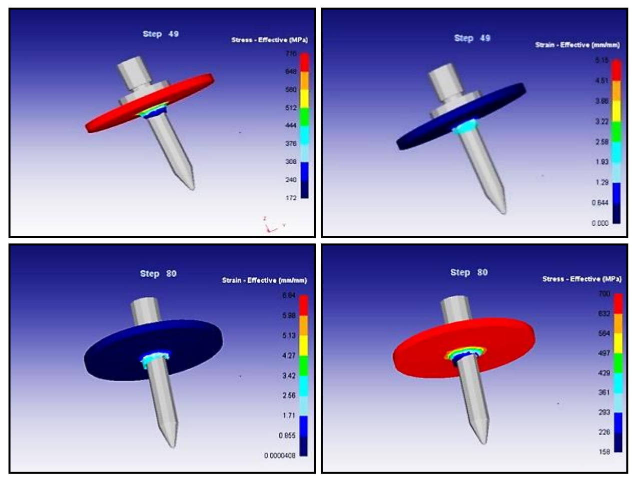

Fig. 6 Stress, strain analysis of HSS tool on AL6061-T6 workpiece at Feed 0.04mm/rev and Speeds 1980 & 1250rpm.

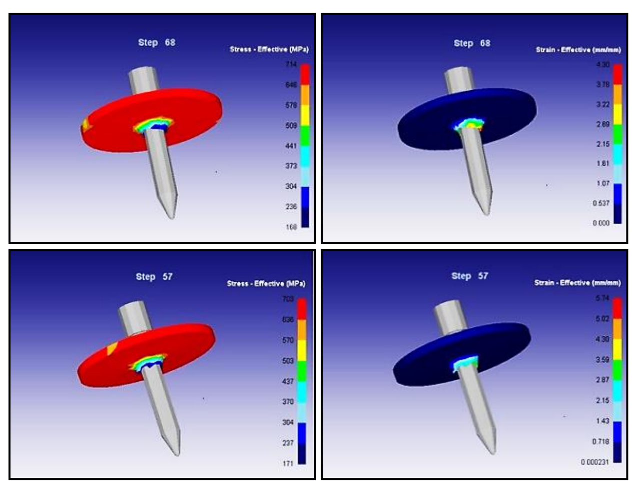

Fig. 7 Stress, strain analysis of Tungsten Carbide tool on AL6061-T6 workpiece at Feed 0.08mm/rev and Speeds 1980 & 1250rpm

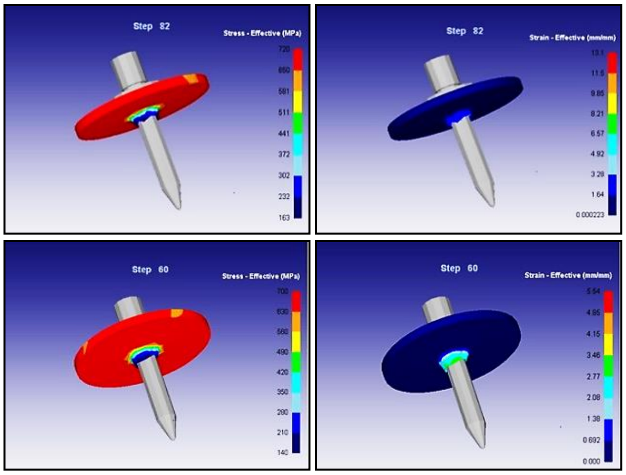

Fig. 8 Stress, strain analysis of Tungsten Carbide tool on AL6061-T6 workpiece at Feed 0.04 mm/rev and Speeds 1980 & 1250rpm

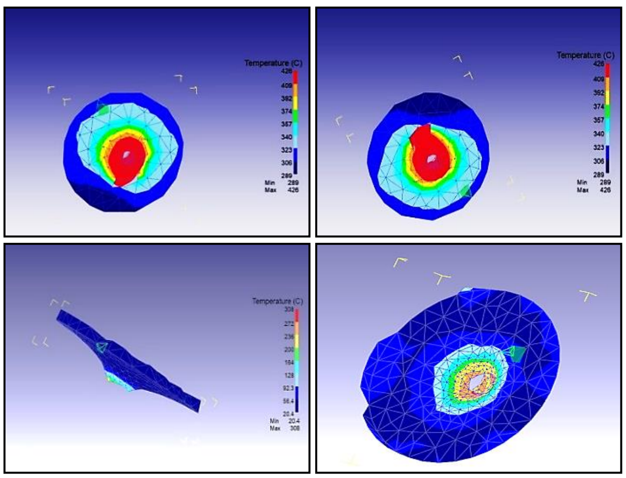

Fig. 9 Temperature distribution and deformation at various speeds and feed rates with HSS and Tungsten carbide tools.

4.1. FEM Analysis for Stress and Strain

The stress and strain of friction drilling can be shown in Figures 5, 6, 7, & 8. Maximum stress is generated at the tool contact zone, and stress minimum at the inside of the surface of the friction drilling hole due to maximum temperature. When speed increases, stress decreases at a constant feed rate. The highest stress of 280MPa can be obtained at a speed of 495 rpm with a feed rate of 0.04mm/rev for the HSS tool, and 230MPa can be obtained at a speed of 495 rpm with a feed rate of 0.04mm/rev with Tungsten Carbide tool.

The minimum stress was observed at 131MPa at a speed of 1980 rpm and fed 0.08mm/rev with the HSS tool and 110MPa at a speed of 1980 rpm feed rate of 0.08 mm/rev with the Tungsten Carbide tool. Similarly, when strain increases with an increase in speed and feed. Hear the highest strain can be observed at 288 at a speed of 1980rpm with a feed of 0.08mm/rev for the HSS tool and 357 at a speed of 1980 rpm feed rate of 0.08mm/rev with the Tungsten Carbide tool.

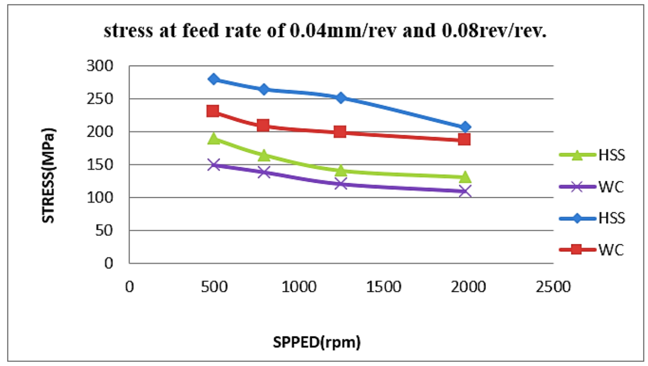

Fig. 10 Speed and feed relationship with stress

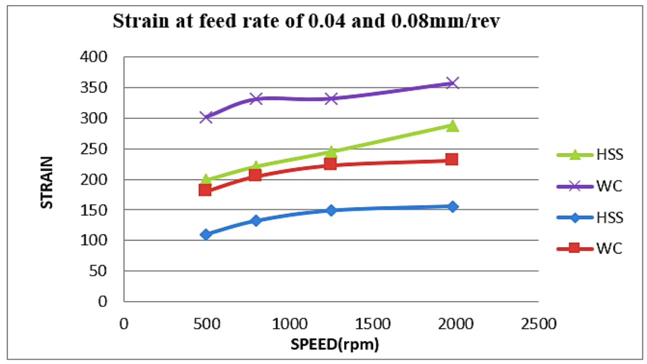

Fig. 11 Speed and feed relationship with Strain

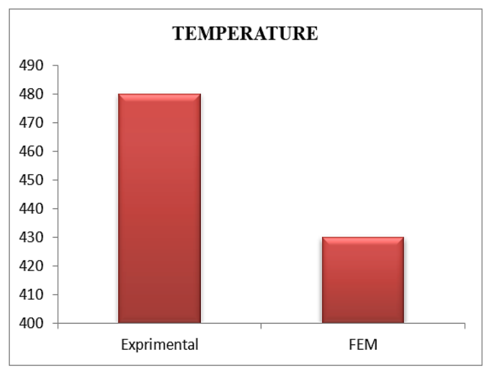

Fig. 12 Compression graph between experimental and FEM simulation with respective Temperature

4.2. FEM Validation

To ensure model fidelity, comparing experimental findings with simulation results is critical. Temperature measurements with HSS and tungsten carbide tools during friction drilling on Al6061-T6 alloy support the FEM model. The experimental result (480 °C) compared to the simulation result (430 °C) in the friction drilling process, which was monitored using thermocouples. In the inside of the hole, the frictional heat created between the tool and workpiece material puts the substance through a visco-plastic stage. Friction drilling begins with heating the workpiece's inner surface, and when it reaches the conical area, the material becomes red hot, causing melting on the workpiece's top surface.

Thermocouples are arranged nearer to the hole's measured temperature at the hole portion. Here compression with simulation results with experimental results of both Tungsten Carbide and HSS tools. The temperature destitution is shown in figure 9. The recorded highest temperatures simulation results from the Tungsten Carbide tool and HSS tool are 415 ˚C & 430 ˚C and the experimental values of the Tungsten Carbide tool and HSS tool is 455 ˚C & 480 ˚C. the compression graph between experimental and FEM simulation as shown in Figure 13.

The deviation observed between simulation and experimental results is ± 6.3%. So that it confirms that the numerical model is working. Temperature values were measured for both the HSS tool and Tungsten Carbide tool at various speeds, i.e. 495, 795, 1250, &1980rpm.

5. Conclusion

This research paper presents the contact area between the rigid workpiece and an unworn tool of a proposed mathematical model with stress and strain properties dependent on speed and feed. The summarized outcomes are as follows:

1. The 3D simulation model was more helpful in finding the material deformation in the friction drilling process. It enabled material flow at various speeds and feed rates with various tool materials. Stress and strain can be measured effectively and cannot be measured experimentally.

2. The maximum stress can be observed at minimum speed and feed rates, while a minimum strain can be observed at decreasing speed and feed rates.

3. When comparing the HSS tool and the Tungsten Carbide tool, maximum stress was generated with the HSS tool at the highest speed and feed rates. Better bushing formation also occurred with the HSS tool.

4. The peak temperature of the workpiece is compared with simulation and experimental results. The highest temperature was obtained experimentally at 480˚C with the HSS tool in and in simulation at 430 ˚C.

References

[1] Mr. Adwait Pohane, Dr. N.K. Kamble and Mr. Y.G. Kamble, "A Review Paper on Friction Drilling Process on Various Materials," *IOSR Journal of Mechanical and Civil Engineering (IOSR-JMCE),* vol. 16, no. 6, pp. 1-4, 2019. Crossref, https://doi.org/10.9790/1684-1606010104

[2] Armin Yazdanshenas, Chung-Hyun Goh, "Rockwell Hardness Testing on an Aluminum Specimen using Finite Element Analysis," *SSRG International Journal of Mechanical Engineering,* vol. 7, no. 4, pp. 1-10, 2020. Crossref, https://doi.org/10.14445/23488360/IJME-V7I4P101

[3] Akshay Potdar and Sagar Sapkal, "Optimization of Friction Drilling Process by Response Surface Methodology," *Advanced Engineering Optimization Through Intelligent Techniques,* pp. 351-359, 2019. Crossres, https://doi.org/10.1007/978-981-13-8196-6_31

[4] Roman Stryczek and Paweł Błaszczak, "*Optimal Feed Rate Control Strategies for Friction Drilling,"* Facta Universitatis Series: Mechanical Engineering, vol. 18, no. 4, pp. 545-564, 2020. Crossref, https://doi.org/10.22190/FUME200510021S

[5] Jun Qu and Peter J. Blau, "A New Model to Calculate Friction Coefficient and Shear Stress in Thermal Drilling," *Journal of Manufacturing Science and Engineering,* vol. 130, pp. 014502-1, 2008. Crossref, https://doi.org/10.1115/1.2815341

[6] Shin Min Lee A, Han Ming Chow B, Fuang Yuan Huang A and Biing Hwa Yan A, "Friction Drilling of Austenitic Stainless Steel by Uncoated and PVD Alcrn- and Tialn-Coated Tungsten Carbide Tools," *International Journal of Machine Tools & Manufacture*, vol. 49, no. 1, pp. 81-88, 2009. Crossref, https://doi.org/10.1016/j.ijmachtools.2008.07.012

[7] Wei-Liang Ku, Han-Ming Chow, Yao-Jang Lin, Der-An Wang and Lieh-Dai Yang, "Optimization of Thermal Friction Drilling Using Grey Relational Analysis," *Advanced Materials Research,* vol. 154-155, pp. 1726-1738, 2010. Crossref, https://doi.org/10.4028/www.scientific.net/AMR.154-155.1726

[8] A. Fernández, L.N. Lopez de Lacalle and A. Lamikiz, "Friction Drilling of Stainless Steels Pipes," *International Conference on Advances in Material and Processing Technologies(AMPT2011)*, 2011. Crossref, https://doi.org/10.1063/1.3552343

[9] S.M. Lee, H.M. Chow, and B. H. Yan, "Friction Drilling of IN-713LC Cast Superalloy," *Materials and Manufacturing Processes*, vol. 22, no. 7-8, pp. 893–897, 2007. Crossref, https://doi.org/10.1080/10426910701451697

[10] N.Srilatha and B.Srinivasa Prasad, "Novel Method of Friction Drilling Technique Review," *AIP Conference Proceedings,* vol. 2200, pp. 020052, 2019. Crossref, https://doi.org/10.1063/1.5141222

[11] Scott F. Miller, Rui Li, Hsin Wang and Albert J. Shih, "Experimental and Numerical Analysis of the Friction Drilling Process," *Journal of Manufacturing Science and Engineering,* vol. 128, no. 3, pp. 802-810, 2006. Crossref, https://doi.org/10.1115/1.2193554

[12] Mehmet Burak Bilgin, Kadir Gök and Arif Gök, "Three-Dimensional Finite Element Model of Friction Drilling Process in Hot Forming Processes," *Journal of Process Mechanical Engineering*, vol. 231, no. 3, 2015. Crossref, https://doi.org/10.1177/0954408915614300

[13] N.Srilatha, Balla Srinivasa Prasad, Karaka and V.V.N.R.Chandra Mouli, "Effect of Temperature on Surface Roughness in Friction Stir Drilling of AL-6061 with Varied Drill Tools," *Materials Today Proceedings*, vol. 62, Part 6, pp. 3909-3915, 2022. Crossref, https://doi.org/10.1016/j.matpr.2022.04.549

[14] Soundararajan V, Zekovic S. and Kovacevic R, "Thermo-Mechanical Model With Adaptive Boundary Conditions for Friction Stir Welding of Al 6061," *International Journal of Machine Tools and Manufacture*, vol. 45, no. 14, pp. 1577–1587, 2005. Crossref, https://doi.org/10.1016/j.ijmachtools.2005.02.008

[15] Chao Y. J, Qi X, and Tang W, "Heat Transfer in Friction Stir Welding-Experimental and Numerical Studies," *ASME Journal of Manufacturing Science and Engineering*, vol. 1251, pp. 138–145, 2003. Crossref, https://doi.org/10.1115/1.1537741

[16] Schmidt H, and Hattel J, "A Local Model for the Thermomechanical Conditions in Friction Stir Welding," *Modelling and Simulation in Materials Science and Engineering*, vol. 13, no. 13, pp. 77–93, 2005. Crossref, https://doi.org/10.1088/0965-0393/13/1/006

[17] Miller SF and Shih AJ, "Thermo-Mechanical Finite Element Modeling of the Friction Drilling Process," *Journal of Manufacturing Science & Engineering*, vol. 129, no. 3, pp. 531–538, 2007. Crossref, https://doi.org/10.1115/1.2716719

[18] R. Kumar and Rajesh Jesudoss Hynes, "Finite-Element Simulation and Validation of Material Flow in Thermal Drilling Process," *Journal of the Brazilian Society of Mechanical Sciences and Engineering*, vol. 40, no. 3, pp. 162, 2018. Crossref, https://doi.org/10.1007/s40430-018-1091-y

[19] Dr. A. Gopichand, M.VeeraBrahmam and D.Bhanuprakash "Numerical Simulation and Analysis of Friction drilling Process for Alumina Alloy using Ansys," *International Journal of Engineering Research & Technology (IJERT)*, vol. 3, no. 12, 2014. Crossref, https://doi.org/10.17577/IJERTV3IS120562

[20] V. Mallikarjuna, Dr. B. James Prasad Rao, G.kishore, "Design and Finite Element Analysis of Crank Shaft by using Catia and Anysys," *SSRG International Journal of Mechanical Engineering*, vol. 4, no. 3, pp. 8-18, 2017. Crossref, https://doi.org/10.14445/23488360/IJME-V4I3P103

[21] Prashant Kumar, Abhishek Bhandari, Sunil Kumar Chaturvedi, "Design and thermal analysis of ic engine piston design using catia and Ansys software," *SSRG International Journal of Mechanical Engineering*, vol. 6, no. 10, pp. 12-19, 2019. Crossref, https://doi.org/10.14445/23488360/IJME-V6I10P103

[22] Narayana Moorthy N and T C Kanish, "The Impact of Process Parameters on Surface Roughness and Bushing in Friction Drilling," *IOP SciNotes*, vol. 1, no. 3, pp. 034402, 2020. Crossref, https://doi.org/10.1088/2633-1357/abc968

[23] Yahya Işık, Hilal Kır, Mesut Mantarlar and Mustafa Yazar, "Analysis of the Fatigue Life of Matrix Elements in the Hole Drilling Process in Sheet Metal Forming Dies," *SSRG International Journal of Mechanical Engineering*, vol. 9, no. 7, pp. 1-9, 2022. Crossref, https://doi.org/10.14445/23488360/IJME-V9I7P101

[24] Mehmet Tuncay Kaya, Alaattin Aktas, Bertan Beylergil and Hamza K. Akyildiz, "An Experimental Study on Friction Drilling of ST12 Steel," *Transactions of the Canadian Society for Mechanical Engineering*, vol. 38, no. 3, 2014. Crossref, https://doi.org/10.1139/tcsme-2014-0023